

A Study of a Low Power Hall Thruster Transient Behavior

W.A. Hargus, Jr. †, N.B. Meezan †, and M. A. Cappelli ‡

Mechanical Engineering Department
Thermosciences Division
Stanford University
Stanford, CA 94305

Abstract

Characterization of the transient behavior of a co-axial xenon Hall accelerator is presented. Electrostatic probes, including floating, grounded, emissive (plasma potential), and swept Langmuir probes, are used to measure the time-average and spectral properties of the plasma both outside and within the acceleration channel. The measurements confirm the existence of low-frequency ($< 100\text{kHz}$) coherent azimuthal drift waves and more stochastic disturbances within the channel. The properties of these disturbances depend on the location within the channel, and where in the current-voltage characteristics the thruster is operating, in agreement with observations in other Hall thrusters documented in the literature. Measurements of the time-average plasma potential indicates that in this particular Hall thruster, the largest axial electric field exists between the channel exit and cathode plane, consistent with recent laser-induced fluorescence measurements in the same device, and coincident with the region of the thruster where there is a negative gradient in the magnetic field. The average azimuthal wave speeds are measured and compared to the $\mathbf{E} \times \mathbf{B}$ drift velocity. The electron temperature is relatively uniform along the discharge, and in the range of 5-10 eV, in qualitative agreement with the observed potential differences between the floating potential and floating emissive probes.

Introduction

Proposals to use crossed-field Hall accelerators as high-performance, high specific impulse electric thrusters for satellite propulsion date back to the early 1960's [1]. Numerous experimental and developmental programs were initiated in the United States shortly afterwards [2-4]. These programs established the basic operating principles of the device. In a crossed-field Hall accelerator, electrons (a large fraction of which are emitted by an external cathode) are magnetized by an applied radial magnetic field (in contrast, the ions, with a significantly lower Hall parameter, are not) and the ions, generated by volume ionization, are accelerated by the electrostatic fields established by the retarded electron flow. In a co-axial Hall thruster design, there is an imposed axial electric field and an applied radial magnetic field. In this configuration, the electrons are constrained to move along the azimuthal coordinate, in the direction of the closed $\mathbf{E} \times \mathbf{B}$ drift (hence the name "closed electron drift accelerator"). It was recognized early on, however, that the electron current comprised too large a fraction of the total discharge current than can be accounted for by classical collisional diffusion and that an "anomalous" cross-field diffusion of electrons was necessary in order to account for the enhanced plasma conductivity. An extensive experimental study by Janes and Lowder [5] drew attention to the presence of weakly turbulent density and field fluctuations which give rise to the cross-field transport. These experiments were subsequently followed by the several studies of Morozov and colleagues in the former Soviet Union [6-8], in which the nature and structure of this turbulent plasma was further resolved and in which the first theoretical analysis of the wave dispersion relations were presented.

The nature of the instabilities that give rise to the unsteady behavior in these co-axial Hall accelerators is strongly dependent on the sign of the axial gradient in the applied magnetic field [6]. There appear to be at least

three principle oscillatory modes present in modern Hall thrusters: (i) relatively low frequency (20-60 kHz) traveling azimuthal drift waves (often mislabeled as "ionization waves") in the regions of the thruster where the axial gradient in the applied magnetic field $dB_r/dz < 0$. These waves are predominant when operating along the ionization portion of the I-V curves and are seemingly damped in the current saturation operating regime, except for regions very near the anode [6] where the wave is excited even in cases where $dB_r/dz > 0$; (ii) moderate frequency (~70-500 kHz) largely turbulent axial waves in the regions where $dB_r/dz > 0$, with frequencies centered at approximately the inverse ion transit times (hence these waves are often referred to as transit-time oscillations in the literature [7]); and (iii) high frequency (~MHz) azimuthal waves, evident very near the "optimum magnetic field," defined as where the discharge current is a maximum for a fixed voltage and mass flow rate [8]. These and other oscillatory characteristics of Hall discharges are reviewed and discussed in a recent paper by Choueiri [9].

The precise role played by the oscillatory and turbulent behavior characteristic of these Hall discharges is qualitatively understood [9]. However, a quantitative mapping of the plasma in terms of the regions of instability and their influence on electron transport requires further careful examination of the time-average and temporally-resolved plasma properties within the ionization and acceleration regions of the discharge. Such knowledge gives physical insight into a range of performance-limiting factors in modern-day thrusters [10].

In this paper, we report on preliminary results of experiments aimed at verifying the transient operating characteristics of a Hall thruster designed and fabricated in our laboratory. The primary goal of our research is to develop and apply spatially-resolved plasma diagnostics for the ionization and acceleration regions in Hall thrusters. Recently, we have reported on the application of laser-induced fluorescence (LIF) to measure the neutral xenon and singly-ionized xenon velocities at the exit plane of a laboratory thruster [11,12]. The development and

† Research Assistant, Student Member AIAA

‡ Associate Professor, Member AIAA

application of advanced diagnostics can provide the data needed to further validate models and detailed simulations of Hall thruster operation. These models are expected to be important in the development of the next generation of thrusters that extend the performance envelope. In the study reported here, we have used a variety of electrical probes to characterize the time-average plasma properties and low-frequency (<100 kHz) disturbances in a laboratory Hall accelerator. Complementary thrust measurements allow for the characterization of thruster performance at the conditions examined. The Hall discharge studied here is not intended to be a prototype for an operational thruster and serves only as a test bed for the development of plasma diagnostic tools. Such tools can yield general, quantitative information on the plasma behavior and can be extended for use on prototype thrusters.

Experimental Description

Hall Accelerator and Test Facility

A detailed description of the Hall accelerator studied here and the facility in which these experiments are carried out is provided in another paper [13]. We provide only a brief description in this paper. The test facility consists of a non-magnetic stainless steel tank approximately 1 m in diameter and 1.5 m in length pumped by two 50 cm diffusion pumps. The base pressure of the facility is approximately 10^{-6} Torr. The background pressure during thruster testing at a xenon flow rate of 2-3 mg/sec is typically 10^{-4} Torr. Although this pressure is an order of magnitude lower than that of Janes and Lowder [5], it is still considerably higher than chamber pressures that are generally acceptable for the collection of reliable thruster performance data [14], and it is expected that the ingestion of background gas very near the exit of this discharge may influence the transient discharge characteristics. The possibility of this effect was a partial motivation for this study.

The Hall accelerator used in this study was constructed in 1995 and is the first attempt at Stanford to build a laboratory model Hall thruster [12]. A detailed description of its design is provided in Ref. 13. The thruster consists of inner and outer magnetic pole-pieces surrounding an insulated acceleration channel annulus 10 mm wide and 15 mm in depth. The radial magnetic field has a maximum value of approximately 100 G at a winding current of 2.0 A, the nominal operating conditions for this study. The cathode, required to neutralize the ion beam and support the necessary electric field, is a commercial hollow cathode (Ion Tech, Inc. model HCN-252). The plane of the cathode is approximately 2 cm downstream of the exit of the discharge. Propellant flow to the thruster anode and cathode sections is controlled by two factory calibrated Unit Instruments 1200 series mass flow controllers.

The accelerator channel has a region in which $dB_r/dz > 0$ ($z < 9$ mm) and $dB_r/dz < 0$ ($z > 9$ mm) [13,15]. As discussed by Morozov [6], the axial variation in the magnetic field has a significant affect on the transitory response of these discharges. In addition, his studies revealed that for discharges in which $dB_r/dz \geq 0$ over the entire channel, the ratio of the average ion current (I_i) to total average discharge current (I_d), $\xi = I_i/I_d$ can exceed 60%. In contrast, when $dB_r/dz < 0$, $\xi \leq 0.4$. The enhanced electron current conductivity is attributed to the instabilities associated with the low-frequency traveling azimuthal drift waves predominant in the region of the discharge where $dB_r/dz < 0$. These disturbances give rise to

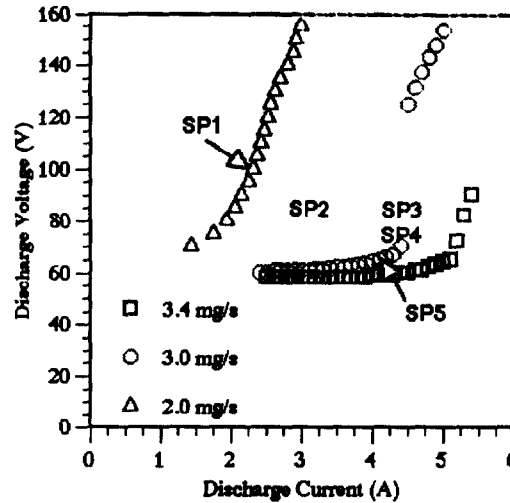


Figure 1. I-V characteristics of the Hall thruster operating on xenon.

equipotential surfaces that connect the exit plane to the anode along which the electrons can migrate [6]. As discussed below, the magnetic field distribution present in our discharge supports the growth of such waves, and gives rise to values of $\xi \sim 0.4$ at the cathode plane under nominal operating conditions. This relatively low value indicates that the thruster is operating at below optimum performance. This is attributed to the shape and strength of the applied magnetic field.

Figure 1 shows a the I-V characteristics typical of this thruster. Unlike the I-V response seen in space-qualified thrusters, we see that the current continues to rise significantly beyond the region of the "knee". In many cases, we do not observe a distinct current saturation region. Two possible explanations for the absence of a distinct saturation in the discharge current are (i) the relatively high background pressure ($\sim 10^{-4}$ Torr), which gives rise to continuous and incomplete ionization resulting from the ingestion of background gas in the chamber; and (ii) the shape and magnitude of the magnetic field. The latter issue is discussed in more detail in Ref. 13, where the performance of this thruster is compared to that of a thruster with a significantly different magnetic field distribution.

Also indicated in Figure 1 are five operating conditions for which a more extensive set of data is gathered. Operating set point SP1 ($V_d = 100V$, $I_d = 2.3A$, $\dot{m} = 2$ mg/sec anode flow rates) represents operation in a near-current saturation mode. Set point SP2 ($V_d = 85V$, $I_d = 3.1A$, $\dot{m} = 2.5$ mg/sec anode flow rates) represents operation just above the knee at a moderate xenon flow rate (entire I-V curve not shown). Set point SP3 ($V_d = 85V$, $I_d = 4.5A$, $\dot{m} = 3$ mg/sec anode flow rates) represents operation at the same voltage as SP2 but at the highest mass flow investigated. Set point SP4 ($V_d = 75V$, $I_d = 3.7A$, $\dot{m} = 3$ mg/sec anode flow rates) and SP5 ($V_d = 65V$, $I_d = 3.35A$, $\dot{m} = 3$ mg/sec anode flow rates) represent operation along the same I-V curve as SP3, but at lower power, closer to and just below the "knee" respectively.

Floating Potential Probes

A number of measurements are made of the floating potential of the plasma along the axial and azimuthal coordinates of the thruster both outside and within the accelerator channel. The floating potential probes consist of a 0.5 mm diameter tungsten wire surrounded by an alumina sleeve oriented such that the axis of the exposed

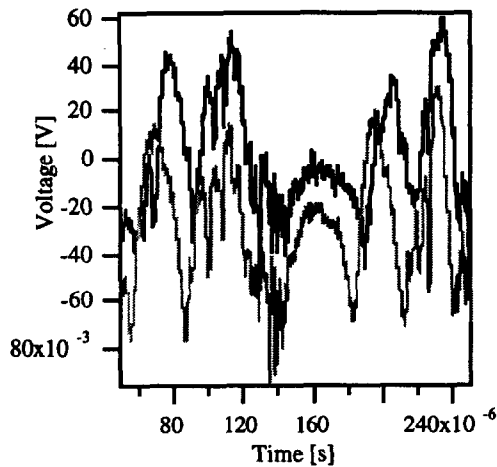


Figure 2. Oscilloscope traces of the signal from two floating potential probes placed 45° apart along the azimuthal direction at the exit of the Hall thruster.

portion of the probe was perpendicular to the axial coordinate of the thruster. The exposed length of the probe was 0.3 cm providing a total probe area of approximately 5 mm². The probe leads were attached to the center pin of a 50Ω co-axial cable, with a grounded outer shield. Co-axial transmission line feedthroughs provided the transfer of the signal through the chamber into a Tektronix model TDS-210 oscilloscope.

For evaluation of DC component and the low frequency (<50kHz) AC oscillations in the floating potential, the signals were terminated with the internal 1 MΩ impedance of the oscilloscope. We note that this termination is likely to make the detection of phase shifts unreliable since the 1 MΩ termination on the oscilloscope causes the co-axial cable to act as a low-pass filter, compromising the frequency response of the system. Verification that the system was adequately capturing the low frequency (<50kHz) AC structure in the signal was performed by comparing the transient signal obtained with a 1 MΩ impedance to that obtained with a 75kΩ and 50Ω terminator on the oscilloscope.

The time-variation in the floating potential is not a measure of the time-variation in the plasma potential. However, it has been shown by Esipchuk et al. [7] that the time-varying component of a floating potential probe is equal to that of a hot emissive (floating) probe in a Hall accelerator. As pointed out in Ref. 7, this implies that the disturbances giving rise to time-varying potentials are isothermal since the differences between the floating and plasma potential are in general proportional to the electron temperature ($\phi_p - \phi_f \sim 2kTe$). We therefore interpret the transient oscillations on the floating potential probes to reflect the spectra associated with transient oscillations in the local plasma potential on the basis of these prior findings.

Azimuthal Wave Speed Detection Probes

The same type of probes described above to detect the floating potential were used to determine the average phase velocity of the azimuthal waves. Two probes were separated by 45° along the azimuthal coordinate midway between the inner and outer insulating walls. In order to achieve a high degree of sensitivity to a wide spectral range, the signals to the oscilloscope were terminated by 50Ω in order to match the impedance of the co-axial transmission line. As a result of this low impedance

termination, the signals do not represent the floating potentials. Instead, the exposed wires behave more like grounded probes. It is therefore difficult to directly relate the amplitude of the fluctuations to the time-variation in a particular plasma property (i.e., plasma potential, density, etc.). It is noteworthy however, to mention that the oscilloscope trace was nearly identical in structure to that of the signal from a probe terminated with 75kΩ, the time average signal of which was close to the floating potential. As a result, we believe that oscillatory signal in these low-impedance traces reflects the oscillatory variation in the floating or plasma potential. Regardless, the primary intention of these measurements was to detect the time delay between the arrival of the disturbances on the two probes. The power spectra from these probes was used to qualitatively interpret the spatial characteristics of the disturbances within the discharge channel.

An example of the oscilloscope traces from the two probes (separated by 45° in the azimuthal direction) placed at the exit plane of the Hall accelerator operating at the set point SP1 is shown in Figure 2. A distinct time delay between the two probe traces is apparent. However, it is also apparent that at this operating set point the disturbance is not of a pure wave, and that the phase delay is not consistent across the entire trace, indicative of a degree of turbulence. In the results presented in the next section, a cross-correlation of the two traces is used to obtain a representative average of the phase delay between the two signals, from which an estimate of the traveling azimuthal wave speed can be derived. The cross-correlation is also used to qualitatively determine the coherence of the waves.

The calculated wave speed, v_p , is expected to be considerably less than the azimuthal drift velocities, $v_d = E_z/B_r$. In prior studies of Hall discharges, measured values of v_p range from 0.2 to 0.8 v_d . This is in agreement with the theoretical analysis of Esipchuk and Tilinin [8] as shown by Choueri [9]. The source of excitation of these waves is the electron drift velocities associated with gradients in the magnetic field and/or plasma density [9].

Hot Probes for Plasma Potential Measurements

Two probes were constructed to measure plasma potentials in the plasma produced by the Hall thruster. The first probe consisted of tungsten wire 0.50 mm in diameter and 5.0 mm in length placed perpendicular to the ion flow. The lead immediately behind the probe was insulated by 1.6 mm diameter alumina tube and shielded instrumentation cable through a vacuum feedthrough and connected to a digital voltmeter.

The first probe is only used to verify the floating potential measurement of the second probe and extends the measurements of the floating potential of the second probe to within a few millimeters of the anode. The second probe is designed to measure plasma potential by heating a 5 mm long tungsten wire filament using a 12V stepdown transformer. The transformer electrically isolates the probe from line voltage (110V) yet allows the probe to be heated such that the thermionic emission of the probe overcomes the impedance of the probe sheath. The probe therefore floats at near the true plasma potential. When the transformer is unpowered, the probe is cold and the entire circuit remains at the local floating potential. The filament was suspended perpendicular to the ion flow by two sections of 22 gauge copper wire sheathed in 1.6 mm diameter alumina tubing. Plasma and floating potentials were measured at the center tap of the

transformer by a digital voltmeter relative to the thruster ground.

Langmuir Probe for Temperature Measurements

A Langmuir probe consisting of a tungsten wire 0.50 mm in diameter and 5.0 mm in length was placed in parallel to the plasma flow. It was swept using a Kepco Instruments BOP72-3 four quadrant power supply. Current flow through the probe was measured using a 10 Ω shunt. The voltage across the shunt was measured using a unity gain high common mode rejection Burr-Brown AN-117 differential amplifier.

The measured current-voltage traces were analyzed using planar probe theory as outlined in Ref. 16. Near the floating potential, the total current collected by a driven probe is given by:

$$I = I_e e^{-e(\phi_p - \phi)/kT_e} - I_i \tag{1}$$

where I is the measured current, ϕ is the probe potential, ϕ_p is the plasma potential, I_e is the electron temperature, I_e is the electron saturation current, I_i is the ion saturation current, k is Boltzmann's constant, and e is the electron charge. The above equation can be rearranged to express the temperature as the inverse of the slope of the measured voltage-current trace.

The interaction between probes and magnetic fields is not well understood. It has been recognized that probes with lengths on the order of the Larmor radius are less affected by magnetic fields, and so the probe length was intentionally short. The probe was further constrained by the length to diameter ratio so that end effects could be neglected.

Thrust Measurements

The thrust stand used in this study has been discussed extensively in the literature [13,14]. It is an inverted pendulum type thrust stand built by the Jet Propulsion Laboratory and loaned to Stanford for the duration of this work by the U.S. Air Force Phillips Electric Propulsion Laboratory. Thrust is determined from the pendulum displacement measured by a linear voltage differential transducer. Calibration is provided by four 5.0 g weights. Thermal drift is minimized by water cooling surfaces exposed to the thruster plume and the portion of the stand that supports the thruster.

For each thrust measurement, the thruster was run for a period of 10-15 minutes to stabilize the thruster operation and to allow the thrust stand reach thermal equilibrium. Subsequently, 3 to 5 measurements of the thrust stand displacement were made, interspersed with induced oscillations to minimize stiction of the thrust stand. All power to the thruster was then turned off and a calibration of the thrust stand followed. Further details on these thrust measurements can be found in Ref. 13.

Results

Measurements of the time-variation in the floating potential were made with low frequency resolution (<50 kHz) within the accelerator channel for the four operating set points described above. A relative measure of intensity of the disturbances along the channel is the probe *voltage modulation*, defined here as twice the calculated standard deviation in the signal traces, ΔV . Figure 3 gives the variation in ΔV along the accelerator channel. We see that in all cases, the low frequency disturbances are uniformly distributed throughout the channel, with the exception of set point SP1, where there

is a noticeable increase in the amplitude of the disturbance (to about 16% of the peak) in the vicinity of the peak in the radial magnetic field. The nature of these disturbances, i.e., whether they are traveling waves or transient, uncorrelated (turbulent) disturbances are determined from the low-impedance terminated probes, as discussed below. The frequency spectra of the disturbances (as detected with the probes terminated with a 50 ohm impedance to match the co-axial line) at various axial positions within the channel are plotted as contour diagrams in Figure 4.

For the set point SP1, which corresponds to the thruster operation in the current saturation regime of the I-V curve, we see that the frequency spectrum is quite broad, with enhanced excitation of relatively low-frequency oscillations (~17kHz) coincident with the region of maximum magnetic field. This result is consistent with the high impedance terminated floating potential data. The relatively low frequencies appear to be characteristic of the so-called "loop" or "circuit" instabilities [9]. The origin of such instabilities are poorly understood, and are known to be quite sensitive to the power supply characteristics. The coincidence between the activity of this mode and the region of highest magnetic field suggests that this instability is associated with the ionization process, and indeed it has been referred to as the "instability in the position of the zone of ionization," in the previous Russian literature as described in Ref. 9. The contour plot for SP1 shows some excitation of frequencies in the 27kHz range.

For set point SP2, which corresponds to operating just above the knee of the I-V curve, we see the emergence of instabilities in the 27kHz frequency range, characteristic of traveling azimuthal drift waves often described in the literature. As mentioned above, this disturbance is slightly

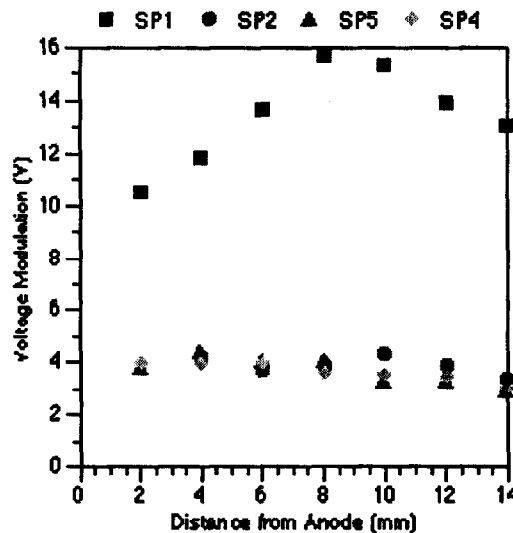


Figure 3. Variation in the voltage modulation as detected from the floating potential probe: squares-SP1; circles-SP2; diamonds-SP4; triangles-SP5.

evident in the case of SP1, although it is masked by the presence of the 17kHz mode. We also note that for this operating condition, that the activity is concentrated mainly near the exit plane ($z > 9$ mm), where the gradient in the magnetic field is negative, i.e., $dB_r(z)/dz < 0$.

The frequency of this apparent azimuthal mode shifts slightly towards higher values (~27-35 kHz) at even higher mass flow rates, as indicated in the contour plot for set

point SP3. Furthermore, we see that this oscillation appears to have spread throughout the entire discharge channel of the thruster. There is little evidence of activity at frequencies $< 20\text{kHz}$.

At the lowest voltage and highest mass flow rates studied (set point SP5), the disturbances in this frequency range are not as strong, are perhaps shifted to slightly lower frequencies, and, are predominantly active near the anode. More interesting is the appearance of a harmonic at approximately 42 kHz .

The nature of these disturbances can be further resolved by use of the two azimuthally separated probes to study the coherence of these waves in the azimuthal direction. Figure 5 shows a cross-correlation of the two signal traces given in Figure 2, taken with two probes separated by 45° in the azimuthal direction at the exit plane of the thruster operating at the set point SP1. The shift in the peak of the correlated spectrum is apparent,

indicating an average phase shift of $4.1 \pm 0.3\ \mu\text{sec}$. This phase shift corresponds to a wave speed of $8.6\ \text{km/sec}$, in the direction of the $\mathbf{E} \times \mathbf{B}$ drift. The easily discernible phase shift indicates that these disturbances are highly correlated, indicative of a coherent traveling azimuthal wave.

Table 1 gives the measured time delay, τ_d , between the signal traces and the calculated variation in the azimuthal wave speed, with axial position for four of the operating set points. In almost all cases, the azimuthal phase shift is difficult to prescribe with certainty in the axial region between 2 and 6 mm from the exit anode (where $dB_r/dz > 0$), as the coherence in the signals is poor. Furthermore, with the exception of set point SP4, the traveling azimuthal wave is clearly excited near the exit plane, where $dB_r/dz < 0$. For set point SP4, the only discernible phase shift is near the exit plane, where there is a fair degree of coherence in the signals.

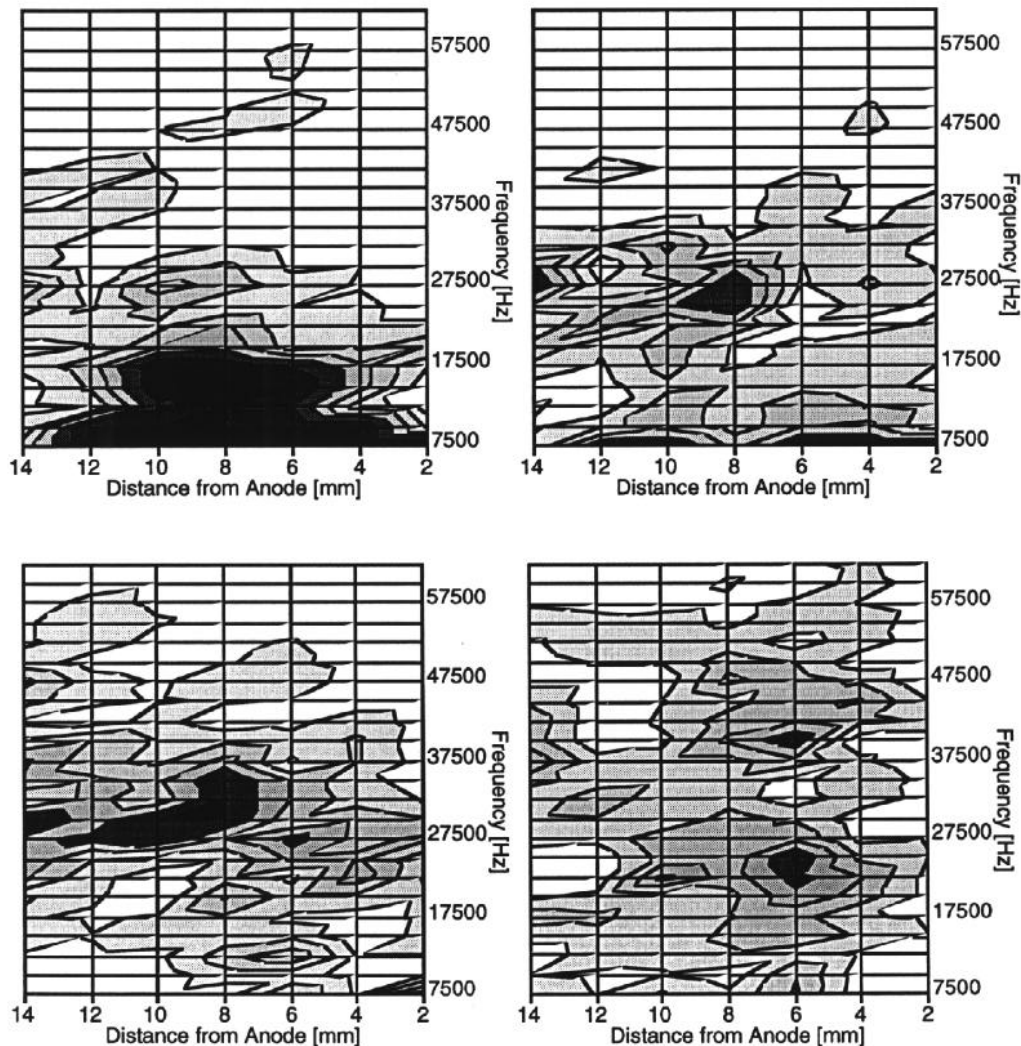


Figure 4. Contour diagrams of the power spectrum of the oscillations detected with the low-impedance probes at various locations within the thruster. The four diagrams refer to the for nominal operating set points: top left-SP1, top right - SP2, bottom left-SP3, bottom right-SP5.

Combining this result with that of the contour diagrams in Figure 4, we can summarize the following: (i) when operating on the current saturation region of the I-V curve, there appears to be a *weak* but very *coherent* traveling azimuthal wave near the exit plane of the thruster. The calculated wave speeds vary between 7-20 km/sec, increasing steadily as the peak in the magnetic field is approached from the exit plane inwards. We also see broader spectral activity (extending to 10 kHz). The strongest instabilities seem to be near the region corresponding to the maximum magnetic field, possibly so-called "loop" instabilities, which appear to be much less coherent than the waves closer to the exit plane in our thruster; (ii) operating closer to the "knee" region, we see the distinct presence of a strong traveling azimuthal wave near the exit plane. The wave speeds are slightly lower than the higher voltage conditions of set point SP1. There is very little high frequency disturbance (>35kHz), and any activity in the region where $dB_T/dz > 0$ appears to be uncorrelated; (iii) operating on the ionization portion of the I-V curve close to the knee, the traveling azimuthal wave is even more pronounced. It seems to extend further into the channel, and the frequencies associated with this wave seem to shift to higher values; (iv) At the low voltage end of the ionization region of the I-V curve, the traveling azimuthal wave is still distinct but present only in the region very near the anode. There is evidence here for some bifurcation of the wave, possibly into the $m = 2$ azimuthal mode.

The measured DC averaged variation in the floating and plasma potential (obtained with the heated emissive probe) with axial position within the discharge and in the near-plume region is shown in Figure 6. The conditions for these measurements correspond to operating set point SP1. Recall that the cathode plane is located at a distance of 2 cm beyond the channel exit or 34 mm from the anode. From these data, we see that there is at most a 10V drop in potential along the channel, and much of the potential drop takes place between the exit and cathode plane. This result is consistent with the ion velocities measured by laser-induced fluorescence (LIF) for similar operating conditions [12]. From the LIF data, the ions are found to have very low energies (typically 2-5 eV) at the exit plane, accelerating to approximately 50eV below the applied potential at the cathode plane. The surprising

result is that a relatively high plasma potential persists well beyond the cathode plane.

The difference between the plasma and floating potential is also depicted in Figure 6. Qualitatively, it is representative of the variation in the electron temperature of the plasma. A direct analysis of the potential that a floating surface will take relative to that of the distant plasma is difficult in this case in that an estimate of the ion flux to the floating probe is required. The ion flux will vary with location within the discharge.

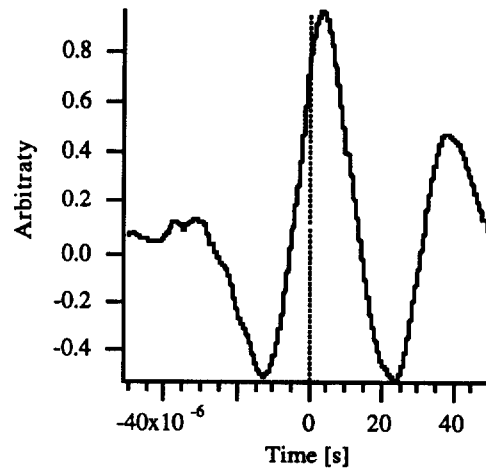


Figure 5. Cross-correlation spectrum of the two oscilloscope signal traces shown in Figure 2 corresponding to the exit plane of the thruster operating at set point SP1.

If the ion flux to the probe is limited by the Bohm velocity (a reasonable assumption inside the channel), then $\phi_p - \phi_f \sim 2.5kTe$. If we assume that the effective electron and ion collection areas to the probe are equal. This estimate suggests that the electron temperature rises from about 8V near the anode, reaching a maximum of 25V at the exit plane. These temperatures are higher than those reported previously [9], and the difference can be attributed to the simple treatment of the ion current collected by the floating probe.

SP1							
time delay (μ sec)	4.1	4.5	2.7	1.8	1.3		
wave speed (km/s)	7.7	7.1	11.8	17.6	24.4		
coherence (poor/fair/good)	good	good	fair	fair	good	poor	poor
distance from anode (mm)	14	12	10	8	6	4	2
SP2							
time delay (μ sec)	8.6	7.5					
wave speed (km/s)	3.7	4.2					
coherence (poor/fair/good)	good	fair	poor	poor	poor	poor	poor
distance from anode (mm)	14	12	10	8	6	4	2
SP3							
time delay (μ sec)	5.7			5.7	4.5		
wave speed (km/s)	5.6			5.6	7.1		
coherence (poor/fair/good)	good	poor	poor	fair	good	poor	poor
distance from anode (mm)	14	12	10	8	6	4	2
SP4							
time delay (μ sec)	9.8						
wave speed (km/s)	3.2						
coherence (poor/fair/good)	fair	poor	poor	poor	poor	poor	poor
distance from anode (mm)	14	12	10	8	6	4	2

Table 1

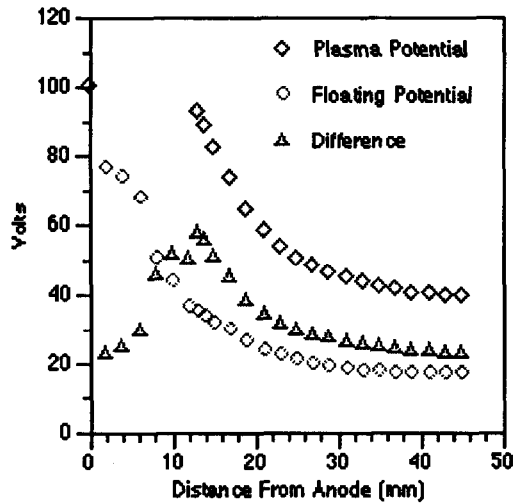


Figure 6. Plasma and floating potential variation and difference along the axial direction for the thruster operating at set point SP1 (100V). The plasma potential data extends from the plume to the exit plane.

A more direct measure of the electron temperature for conditions of set point SP1 was provided by the swept Langmuir probe. Figure 7 shows the corresponding variation in the electron temperatures with axial distance from the anode. We see that the temperatures derived from the Langmuir probe are considerably lower than that derived from the differences between the floating and plasma potential, and are in general qualitative agreement with the temperature measurements of Bishaev et al., [17] as given in Ref. 9. For the case shown in Figure 6, the Langmuir probe data indicates that the temperature rises from about 8eV at the cathode plane to 10eV near the exit plane.

Table 2 contains previously taken thrust measurements made on the Hall accelerator corresponding to several operating set points. From the measured thrusts and mass flows, mean propellant exit velocity, specific impulse, and thrust efficiency were computed [13]. It should be noted that these quantities are calculated using total mass flow and total system power. Total system power includes power dissipated in supporting the cathode discharge and producing the magnetic field. Adjustment is not made to account for cathode and magnetic circuit inefficiencies. However for all but one case, a minimum of 90% of the mass flow and 80% of the power dissipated was in the main discharge of the Hall thruster.

Comparing Figure 4 to the available thrust data for set point conditions SP1, SP3, and SP5 several trends are apparent. First, the Hall discharge is not operating in a particularly efficient regime. Difficulties with the thruster [13] and the necessity of inserting probes into the discharge required that the thruster be operated at lower than optimal voltages. These low voltages invariably

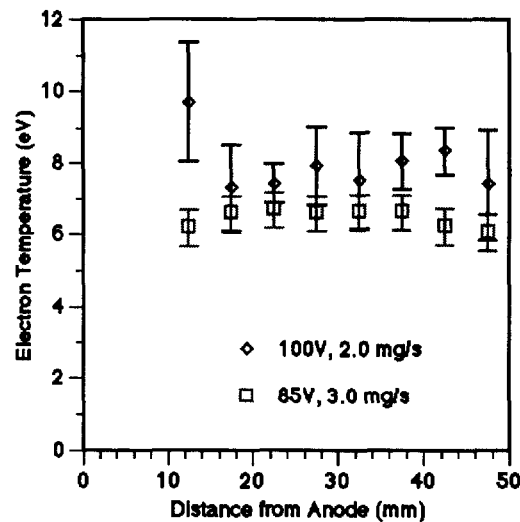


Figure 7. Swept Langmuir probe temperature data.

result in low thrust efficiencies. Second, SP1 and SP3 are significantly more efficient test points than SP5 by nearly a factor of three. Of these conditions, only SP5 exhibits significant higher frequency features. Although SP2 thrust data is not available, it too contains significant high frequency structure in Figure 4. This suggests a relationship between the apparent bifurcation of SP5 and its low efficiency.

Discussion

The results of our study are consistent with those of previous researchers [5-8]. We see clear evidence of the existence of traveling azimuthal waves that are excited predominantly near the exit plane of the Hall thruster in the vicinity where there is a negative gradient in the magnetic field. The strength of these relatively low frequency (~27 kHz) waves depends on the operating conditions, in particular, where in the region of the I-V curve the discharge is sustained, as seen previously [6]. These traveling azimuthal waves do not appear to be excited near the anode. Transient activity in this region where there is a positive gradient in the magnetic field seems to be more turbulent.

Where there was clear evidence for the coherence of these waves, an indirect estimate of the electric field can be obtained from the derivative of the time-varying potential and the measured of the wave speed. At the exit plane of the thruster operating at set point SP1, we estimate the maximum azimuthal electric field to be $E_{\phi} \sim 1$ V/cm. This can be compared to the axial field at the exit plane, $E_z = 45$ V/cm, estimated from the axial variation in the plasma potential, as shown in Figure 6. A measure of the plasma density fluctuations would allow us to combine these results to determine the effective Bohm coefficient which characterizes the cross-field electron transport [5]. Using the measured wave speeds, which have much uncertainty in them, to evaluate the azimuthal field is tenuous. A closely-space dual probe is a better approach

Mass Flow (mg/s)	Anode Flow (mg/s)	Discharge Voltage (V)	Current (A)	Thrust (mN)	(+/-) (mN)	Mean V (m/s)	Specific Impulse (s)	Eff.	Specific Power (MJ/kg)
3.03	2.93	63	2.91	8.04	1.7	2653	270	0.04	78
3.03	2.93	85	4.35	17.7	0.5	5832	594	0.12	142
2.05	1.95	100	2.22	11.0	0.2	5341	544	0.11	135

Table 2

[5]. The probes in the dual-probe studies presented here were separated by too far a distance to use their differences to estimate the electric field.

The azimuthal wave speeds measured near the exit plane (~ 10 km/s) during operating set point SP1 can be compared to the $E \times B$ drift velocity, which for this case is 4.5×10^4 m/s. From Table 1, we see that the ratio v_p / v_d is approximately 0.2 - 0.4, in good agreement with that observed by others [9]. It is interesting to note that the data in Table 1 shows the measured wave speed to increase along the direction where the ratio of E_z/B decreases. This result has not been discussed in the prior literature. In essence, there is no unique value of the ratio v_p / v_d and it depends on the location within the thruster. This suggests that these waves are not directly excited by the azimuthal electron drift, but, rather, are more closely connected to the drift velocity associated with spatial gradients in the plasma properties.

The wavelengths of these traveling azimuthal waves can be estimated from their frequency and phase separation as measured by the probes separated by 45° . The traces in Figure 4 show that these azimuthal disturbances have wavelengths comparable to the channel circumference, confirming that indeed these disturbances correspond to the $m = 1$ (fundamental) azimuthal mode.

The difference between the measured floating and plasma potential, which is representative of the electron temperature, is a maximum close to where the magnetic field is a maximum in the channel. The previous LIF data (and the spatial variation in the plasma potential) show that the ionization zone and the acceleration zone are distinctly separated in this device. Also, it is apparent that the ions leave the exit of the channel with very low velocities, and gain their energy over a distance of about 2 cm outside the thruster, between the exit plane and cathode plane.

Future studies will be aimed at developing a more refined understanding of the structure of these low frequency azimuthal modes, and in extending the investigations to the transit-time and high frequency azimuthal oscillations as we develop a discharge that can operate closer to the "optimum" range of magnetic fields. In particular, non-intrusive, spatially and time-resolved laser measurements will be developed to replace the probe methods that we have employed in this study.

Acknowledgment

This work is supported by AFOSR. W.A. Hargus, Jr. is supported under the Air Force Palace Knight Program.

References

1. E.C. Lary, "Ion Acceleration in a Space-Charge Neutral Plasma," UAC Research Laboratory Report UAR-A125, June, 1962.
2. G.R. Seikel and E. Reshotko, "Hall Current Ion Acceleration," Bull. Am. Phys. Soc. 7, 414, 1962.
3. E.C. Lary, R.G. Meyerand Jr., and F. Salz, "Ion Acceleration in a Gyro-dominated Neutral Plasma: Theory and Experiment," Bull. Am. Phys. Soc. 7, 441, 1962.
4. E.A. Pinsley, C.O. Brown, and C.M. Banas, "Hall Current Accelerator Using Surface Contact Ionization," J. Spacecraft 1, 525, 1964.
5. G.S. Janes and R.S. Lowder, "Anomalous Electron Diffusion and Ion Acceleration in a Low-Density Plasma," Phys. Fluids 6, 1115, 1966.
6. Morizov, A.I., Y.V. Esipchuk, A.M. Kapulkin, V.A. Nevroskii, and V.A. Smirnov, "Effect of the Magnetic Field on a Closed-Electronic-Drift Accelerator," Sov. Phys. - Tech. Phys. 17, 482, 1972.
7. Y.B. Esipchuk, A.I. Morozov, G.N. Tilinin, and A.V. Trofimov, "Plasma Oscillations in Closed-Drift Accelerators with an Extended Acceleration Zone," Sov. Phys. - Tech. Phys. 18, 928, 1974.
8. Y.B. Esipchuk and G.N. Tilinin, "Drift Instability in a Hall Current Plasma Accelerator," Sov. Phys. - Tech. Phys. 21, 417, 1976.
9. Choueiri, E.Y., "Characterization of Oscillations in Closed Drift Thrusters," AIAA-94-3013, 30th Joint Propulsion Conference, June 27-29, 1994, Indianapolis, IN.
10. V.I. Baranov, Y.S. Nazarenko, V.A. Petrosov, A.I. Vasin, and Y.M. Yashnov, "Theory of Oscillations and Conductivity for Hall Thrusters," AIAA 96-3192, 32nd Joint Propulsion Conference, July 1-3, 1996, Lake Buena Vista, FL.
11. Cedolin, R.J., W.A. Hargus, Jr., R.K. Hanson, and M.A. Cappelli, "Laser Induced Fluorescence Diagnostics for Xenon Hall Thrusters," AIAA-96-2986, 32nd Joint Propulsion Conference, July 1-3, 1996, Lake Buena Vista, FL.
12. Cedolin, R.J., W.A. Hargus, Jr., R.K. Hanson, and M.A. Cappelli, "Laser Induced Study of a Xenon Hall Thruster," AIAA 97-3053, 33rd Joint Propulsion Conference July 6-9, 1997, Seattle, WA.
13. Hargus, Jr., W.A., R.J. Cedolin, N.B. Meezan and M.A. Cappelli, "A Performance Study of a Low Power Hall Thruster," AIAA 97-3081, 33rd Joint Propulsion Conference July 6-9, 1997, Seattle, WA.
14. T. Randolph, V. Kim, H. Kaufman, K. Korzbusky, V. Zhurin, and M. Day, "Facility Effects on Stationary Plasma Thruster Testing," IEPC-93-93, 23rd International Electric Propulsion Conference Sept., 1993, Seattle, WA.
15. W.A. Hargus, Jr., N.B. Meezan, and M.A. Cappelli, "Transient Behavior of a Low Power Hall Thruster," AIAA-97-3050, 33rd Joint Propulsion Conference July 6-9, 1997, Seattle, WA.
16. M. Mitchner and C.H. Kruger, *Partially Ionized Gases*, J. Wiley and Sons, New York, 1973.
17. A.M. Bishaev, V.M. Gavryushin, A.I. Burgova, V. Kim, and V.K. Kharchvnikov, "The Experimental Investigations of Physical Processes and Characteristics of Stationary Plasma Thrusters with Closed Drift Electrons," RGC-EP 92-06, 1st Russian-German Conference on Electric Propulsion Engines and their Technical Applications, Giessen, Germany, 1992.